



This is an extended version of the paper presented in SEE7 conference, peer-reviewed again and approved by the JSEE editorial board.

Analytical and Experimental Seismic Evaluation of Confined Masonry Walls Retrofitted by Steel-Fiber and Polypropylene Shotcrete

Sadegh Dardaei^{1*}, Hamzeh Shakib², Mohammad Khalaf Rezaei³, and Mehran Mousavi³

1. Assistant Professor, Faculty of High Technologies, Tarbiat Modares University, Tehran, Iran,
* Corresponding Author; email: dardaei@modares.ac.ir
2. Professor, Department of Civil and Environmental Engineering, Tarbiat Modares University, Tehran, Iran
3. M.Sc. Student, Department of Civil and Environmental Engineering, Tarbiat Modares University, Tehran, Iran

Received: 10/09/2015

Accepted: 16/12/2015

ABSTRACT

This paper presents experimental and analytical results of in-plane behaviour of confined URM walls retrofitted using steel-fiber and polypropylene shotcrete. In this paper, the experimental program consists of testing three CURM walls. The first specimen wall was tested as a reference wall without any retrofitting. The second and third specimens were retrofitted by using a 50 mm thick layer of steel-fiber and polypropylene-fiber shotcrete on one side in order to compare the behavior of them. The stiffness, shear strength, ductility, and failure mode of the wall specimens were determined and compared. The comparison of the tests results indicated that the shear capacity of the retrofitted walls with mesh-reinforced shotcrete and polypropylene shotcrete increased about 92% and 87%, respectively, compared to unretrofitted wall. Therefore, using steel-fiber was found to have considerable effect on the strength as well as the ductility of the wall compared to polypropylene. An analytical study was adapted based on micro finite element modelling to calibrate the behavior of the numerical models with the experimental walls in terms of shear capacity and cracking pattern. The analytical results show a reasonably agreement with the experimental data.

Keywords:

Confined masonry wall;
Seismic retrofitting;
Mesh-reinforced
shotcrete; Steel-fiber;
Polypropylene-fiber;
Micro modelling

1. Introduction

Owing to high seismic mass, low tensile strength and low ductility, Confined Unreinforced Masonry (CURM) walls as a system element of the masonry building suffered considerable damage in the past earthquakes. To improve the seismic performance of the masonry building against earthquake, a key objective is to improve the in-plane behavior of the wall. An extensive effort has been devoted to propose the seismic retrofitting of the confined

URM walls in order to improve the performance of the retrofitted masonry walls with different strengthening techniques in the recent years [1-3]. Mesh reinforced shotcrete has the wide application method on seismic retrofitting of confined URM walls. In this method, a mesh of reinforcing bars performs onto the surface of masonry wall, then shotcrete overlay spray on it. The thickness of concrete layer can be determined by seismic demand. In general, the

overlay thickness is at least 60 mm. To assure the consistency of the deformations of wall and shotcrete layer, steel mesh should be appropriately anchored to the wall. This retrofitting method significantly increased both strength and ductility of the wall because of the bond effect of reinforcing bars, which affects the crack distribution in the masonry wall [1, 2, 4, 5]. Shear strength of the retrofitted wall is calculated by summation of each component of the strengthened wall such as masonry wall and reinforced concrete layer [6]. On the other hand, the strength and ductility of the steel-fiber concrete has been demonstrated in the studies reported by Ezeldin and Balaguru [7], Bencardino et al. [8], Beddar [9]. Brick masonry wall is a non-elastic, non-homogeneous and anisotropic building material, which consists of masonry units and mortar [10]. Mechanical behavior of brick masonry is influenced by the mechanical behavior of the constituent materials are brick and mortar [11]. The large number of parameters, like anisotropy, material properties of the units and mortar, arrangement of bed and head joints, and quality of workmanship, makes the simulation of masonry structures extremely difficult. Based on these considerations, researchers have provided micro modeling techniques for the analysis of masonry structures. In this method, units and mortar in the joints are represented by continuum elements whereas the unit-mortar interface is represented by discontinuous elements [12-14]. The necessary experimental data must be obtained from laboratory tests in the constituents and small masonry samples. The present study is a numerical and experimental investigation of confined unreinforced masonry walls retrofitted by steel-fiber shotcrete (SFS-W) and polypropylene fiber shotcrete (PFS-W). Finally, the behavior of non-retrofitted and retrofitted confined URM walls was compared. The SFS-W specimen provided better seismic performance in comparison to PFS-W specimen. In this work, in order to calibrate numerical results, a finite element modeling analysis based on micro modeling was also carried out under monotonic loading to achieve an accurate mechanism behavior of the walls. The numerical analyses were compared with the experimental observations.

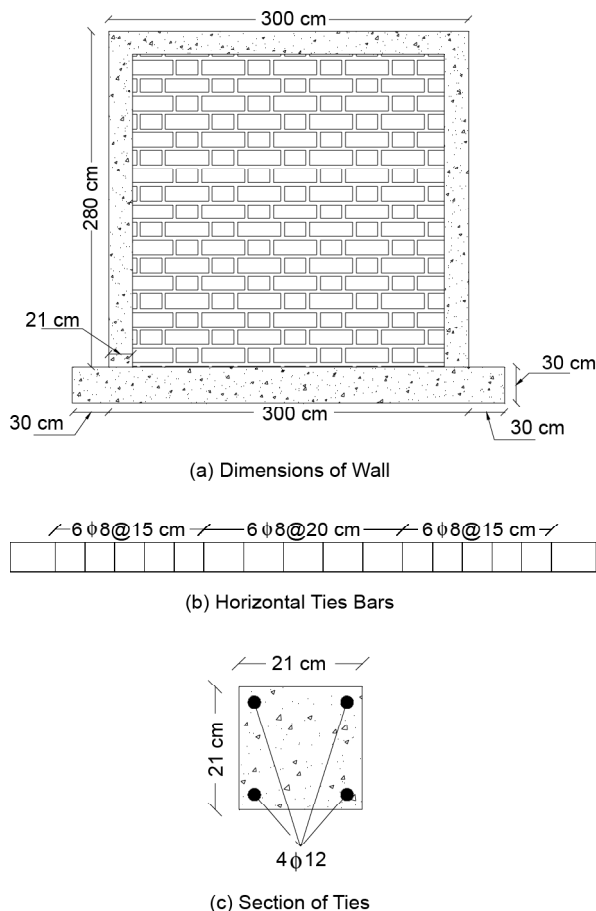
2. Experimental Program

The full-scale masonry walls with nominal

dimensions of $2600 \times 2600 \times 220$ mm were tested to investigate the effects of using steel-fiber and polypropylene-fiber shotcrete on the seismic behavior of confined URM walls. The first reference wall consists of a single-story clay brick panel confined by 210×210 mm RC bond-beams and tie-columns. The dimensions of clay bricks was $210 \times 105 \times 50$ mm. The solid clay brick masonry walls were constructed in Flemish bond brickwork by experienced brick layers with approximately 17 mm thickness mortar joints. Because of poor workmanship of RC members, it was assumed that the concrete have a compressive strength equal to 15 MPa. The RC members have four longitudinal reinforcement bars with 12 mm diameter and reinforcement ties with a diameter of 8×150 mm. The lower RC bond-beam is restrained against horizontal and vertical displacements. However, the upper one transfers static monotonic lateral displacement load. All of the specimens are tested at an age of 28 days. In order to construct the lower tie beams on the strong floor of the laboratory, a steel plate with dimensions of 3600 mm length, 300 mm width and a thickness of 10 mm was fixed on the laboratory's strong floor by high strength steel bolts of 32 mm diameter. The dimensions of the confined URM walls and ties used were outlined in Figure (1). To prevent the probable sliding of lower reinforced concrete tie, angles of $100 \times 100 \times 10$ mm were welded to the plate as shear connectors. All the bricks were pre-soaked to decrease water absorption from the mortar joints to improve the bond strength at the brick-mortar interface [15]. In order to improve the connection between the bricks and the concrete ties, the masonry walls were initially constructed prior to the construction of the ties. Prior to applying the shotcrete, the walls surface was brushed to remove any loose material. Besides, the surface of the walls was completely wetted prior to applying the shotcrete to increase cohesion between the walls and the shotcrete layer [4-5]. The concretes mixture proportion used in this study was prepared in Table (1). For both retrofitted specimens, first, one layer of steel bar mesh of ribless-bar type with diameter of 6 mm at distance of 150 mm was fixed into the drilled holes created on the ties and foundation with a depth of 60 mm and a diameter equal to twice the diameter of the steel mesh bar. The steel mesh has 25 mm distance from the surface

Table 1. Concrete mix design.

	Fiber (kg)	Water (kg)	Cement (kg)	Sand (kg)	Gravel (kg)	Strength (MPa)
Ties and Foundation	---	240	285	860	900	15
Polypropylene-Fiber Shotcrete	10.5	260	420	1228	527	25
Steel-Fiber Shotcrete	42	260	420	1228	527	25

**Figure 1.** Unreinforced masonry wall.

of the wall, approximately. Then, twelve U-shaped shear dowels with a diameter of 10 mm at distance of 600 mm were used to increase integration between the wall and the shotcrete layer. The thickness of the shotcrete layer was about 50 mm. Figure (2) illustrates the details of the retrofitting procedure of the walls.

3. Material Properties

The material properties of the confined URM walls were obtained from the simple component tests specified by ASTM standard. The average compressive strength of the solid clay bricks tested on 5 specimens in accordance with ASTM C67-02C was 24.7 MPa. Mortar with a mix ratio of one part

cement to five parts sand (by volume) with approximate thickness of 17 mm was used due to the prevalence of such construction in old masonry buildings. The water content of the mortar was adjusted to achieve a workable material. The average compressive strength of the mortar tested on five specimens in accordance with ASTM C109/109M-99 [16] was 16.16 MPa. The compressive tests were conducted in accordance with ASTM [18] (ASTM C39) on six cylinder specimens (300 mm height and 150 mm diameter) for tie elements and shotcrete layer concrete. In-situ bed joint shear strength test was carried out on three specimens in accordance with ASTM C1531-02A [17]. The average bed joint shear strength was 0.5 MPa. To determine the mechanical properties of the reinforcing tie bars, UTM devices were used. In accordance with ASTM-A615M standard, the diameter used for the calculation of the yield stress and the ultimate diameter were calculated based on the steel density. A similar mix proportion was also used for the shotcrete layer with polypropylene concrete and steel-fiber concrete (in terms of the cement-sand-gravel-water ratio), but the only difference was the addition of the steel-fiber and polypropylene. The ratio of steel-fiber and polypropylene-fiber in concrete was assumed 10% and 2.5% of the cement by weight respectively [7-9]. The shape and properties of the steel-fiber and polypropylene-fiber outcome in Figure (3) and Table (2).

4. Test Setup and Loading Arrangements

All the specimens were subjected to in-plane displacement controlled cyclic loading by means of hydraulic rams attached to the reaction frame with a simultaneous constant gravity load. The displacement pattern used in the tests is shown in Figure (4). The loadings consisted of two loading cycles at each drift level for all the walls. The nominal vertical load was 10 kN, corresponding approximately to the load of a wall in a one story building with a light roof. The walls were fixed to the floor but free to



Figure 2. Retrofitting procedure.

Table 2. Propertice of fibers.

	Length (mm)	Length of End Hook (mm)	Tensile Strength (N/mm ²)	Diameter (mm)
Steel-Fiber	53 ± 2.5	6	>1.2	0.8
Polypropylene-Fiber	60	---	0.24	0.97

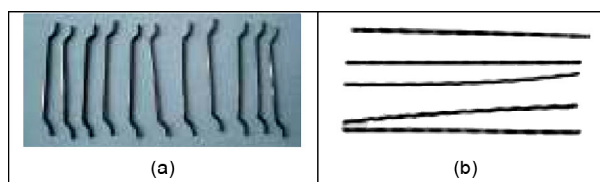


Figure 3. Steel fiber and polypropylene-fiber; a) steel-fiber, b) polypropylene-fiber.

laterally displace and rotate at the top. The horizontal displacement was measured at the top transfer beam with a horizontal transducer. The loading procedure had two phases and consisted of a series of force and displacement-controlled cycles. Before the first

cracks, the loading procedure was force-controlled and consisted of incrementally increasing, single, fully reversed cycles. Then, the loading procedure was changed to displacement-controlled and consisted of a number of steps. The selected test method was

planned to produce data that suitably describe the elastic and inelastic cyclic properties of the walls, which is expected in earthquake loading. The location of the test instruments are shown in Figure (5). Four LVDTs measured the horizontal and vertical in-plane displacements relative to the laboratory strong floor to monitor the probable sliding or uplift of the foundation. The horizontal displacement of the wall was measured at the

bottom of the top tie-beam with a horizontal transducer.

5. Discussion of the Test Results

This section pertains to the experimental observations regarding the behavior, crack pattern, and failure mode of the tested walls subjected to cyclic loading. Figures (6) and (7) present the failure modes and the hysteresis behavior of all specimens respectively. As it is observed in Figure (6a), the confined URM wall had 148 kN shear capacity at 5 mm displacement at the top of wall. The wall had an almost linear behaviour up to approximately 90 kN, at a lateral displacement of 1 mm. In this experiment, the initial horizontal cracks occurred in the junction of the tie-column and foundation on either side. Therefore, the failure mode of the non-retrofitted confined URM wall was bed joint sliding. The failure mode of this wall occurred at a lateral displacement of 5 mm due to the damage near the horizontal crack as shown in Figure (7a). Figure (7 b) and (7c) show the hysteresis behavior of the retrofitted specimen walls with



Figure 4. Position of LVDT.

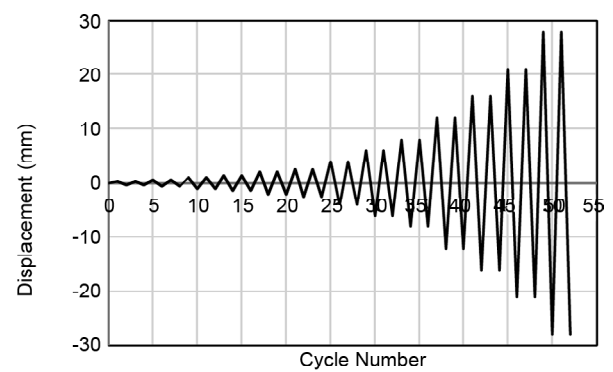
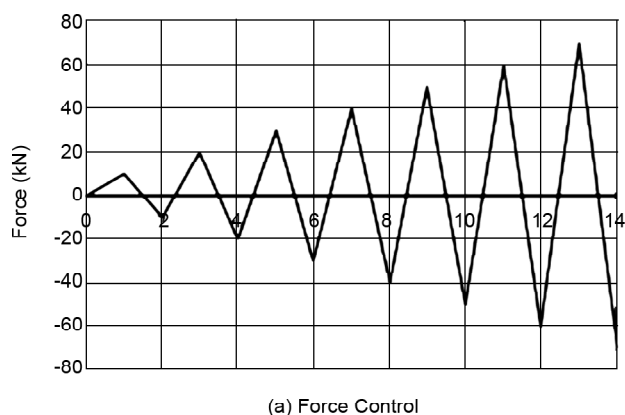


Figure 5. Time history for the cyclic loading tests.



Figure 6. The crack patterns of the walls under cyclic loading.

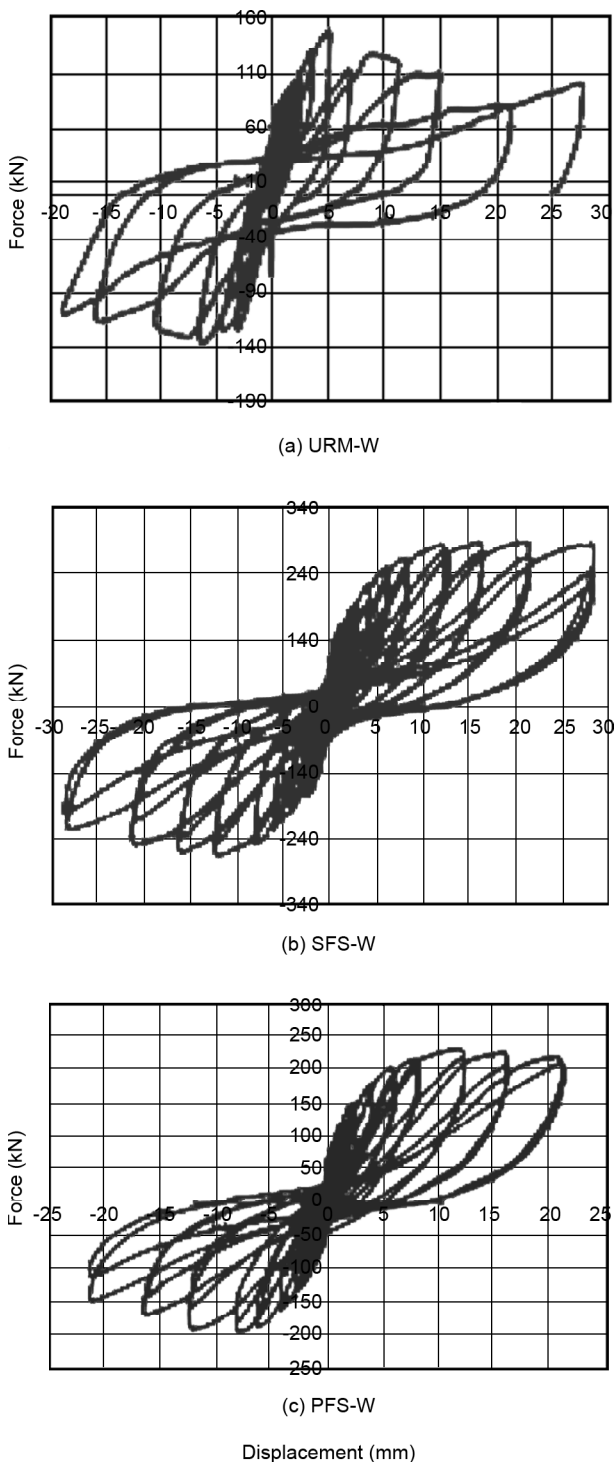


Figure 7. The hysteresis response of the tested walls under cyclic loading.

steel-fibre shotcrete and polypropylene-fiber shotcrete, respectively. Using reinforced concrete layer improves the behavior of the wall and consequently increases the shear capacity and changes the failure mode of the wall in comparison with the URM wall. In both retrofitted walls, a crack was created between the masonry wall and the lower tie-beam denoting the rocking failure

mode of the retrofitted wall. The experimental model indicates that the horizontal crack developed over the whole wall length and detached the wall from the lower tie-beam. The crack width increased by continuous loading cycles and the steel mesh bars that were restrained to the lower tie beam prevented more widening of the cracks width under tension stresses Figures (6b) and (6c). The rocking movement of the walls was associated with toe crushing of the wall at larger displacements. An inclined crack percolated into the foundation and caused damage. The failure mode of these walls can be considered as rocking mode of failure. The experiments suggested acceptable performance with the ultimate strength of 250 kN and 231 kN in lateral displacement of 28 mm and 11.2 mm for both SFS-W and PFS-W specimens, respectively as shown in Figures (7b) and (7c). Therefore, adding mesh-reinforced shotcrete layer increased integrity, shear capacity and energy dissipation. On the other hand, the longitudinal bars of the tie-columns were not under much tensile stress. However, the vertical bars of the steel mesh in the junction of the foundation deformed under high tensile stress. According to the experimental results, the retrofitted walls had much higher shear strength than URM wall with increases of 98% and 87% for SFS-W and PFS-W, respectively as outlined in Table (3). The force-displacement responses of the retrofitted walls are shown and compared with the unretrofitted walls in Figure (8). The shear capacity curves are plotted according to FEMA-356. The results indicated that using steel-fiber increases the shear strength of the wall up to 5.4% compared to polypropylene-fiber. Therefore, using steel-fiber had better performance on the strength, stiffness and ductility compared to the polypropylene-fiber. The hysteresis

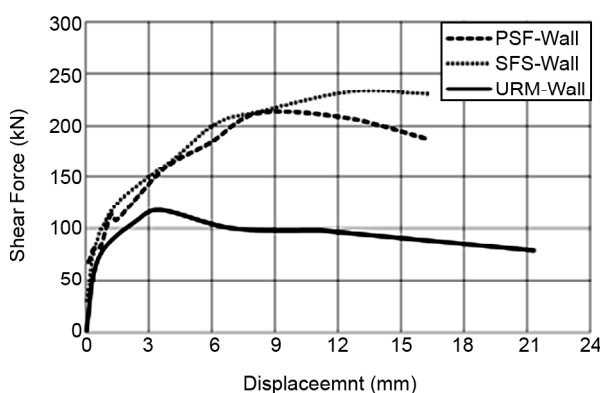


Figure 8. The shear capacity curves of the experimental walls.

Table 3. The capacity and failure mode of unretrofitted and retrofitted URM walls under cyclic loading.

Specimens	Ultimate Strength		Shear Capacity		Increase in Strength (%)	Initial Stiffness $k_i \left(\frac{kN}{mm} \right)$	Failure Mode
	Strength (kN)	Dis. (mm)	Strength(kN)	Dis. (mm)			
URM-W	148	5	117.5	3.58	---	176	Sliding
SFS-W	250	28	233	12.7	87	925	Rocking
PFS-W	231	11.2	221	9.2	98	890	Rocking

characteristics of all specimens are presented in Table (3). The nonlinear behavior of the masonry walls was determined by the idealization of their actual behavior with a bilinear curve.

6. Analytical Results

A pushover analysis is performed to obtain the crack pattern, distribution of the maximum and minimum principal stresses and the force-deformation curve (i.e. capacity curve). Finite element method, particularly detailed micro modeling, was adopted for numerical simulation of the masonry walls. The mortar, brick units and mortar/brick interface were modeled separately. The mortar/brick unit interface was lumped into a zero thickness interface element. Brick units and mortars were modeled with continuum elements. For pushover analysis of a confined masonry wall, a monotonic lateral load should apply on the top of the model based on the ATC-40 requirements. This guideline does not recommend any other load pattern to apply on one-story buildings. The Newton-Raphson iteration method is used. The augmented lateral displacement load is applied at the upper RC bond-beam from left to right after the gravity load analysis is performed. The horizontal loads were applied by means of controlled displacements induced through a hydraulic jack that was placed on a top corner of the wall. The model used for RC members in this study is Concrete Damaged Plasticity (CDP) that developed by Rabotnov and Kachanov [7-9]. The model is a plasticity-based, continuum damage model for concrete. It is assumed that the main two failure mechanisms are tensile cracking and compressive crushing of the concrete material. The evolution of the yield (or failure) surface is controlled by two hardening variables, linked to failure mechanisms under tension and compression loading, respectively. The model assumed that the uniaxial tensile and compressive response of concrete is characterized by damaged plasticity, as shown in Figure (9).

Reinforcement bars were independently modelled as a unidirectional element and embedded inside the concrete material. The steel material was defined with plastic material model with stress-strain curve of Park [?]. The mortar units were modelled by concrete damage plasticity (CDP) model. The behavior of the mortar under tension stress was considered to have the strain softening that was associated with the localization of a single crack and a corresponding sharp tensile stress release [23]. The failure of the brick units was modelled by Mohr-Coulomb material model. The crack patterns and failure modes of the numerical analyses were compared with the experimental results illustrated in Figure (10). As it can be observed, the crack pattern and damage of the numerical models have good agreement with the experimental results. It can also be observed in Figure (11) that the initial and post-yield stiffness and the shear strength of the numerical analyses are in close agreement with the test results.

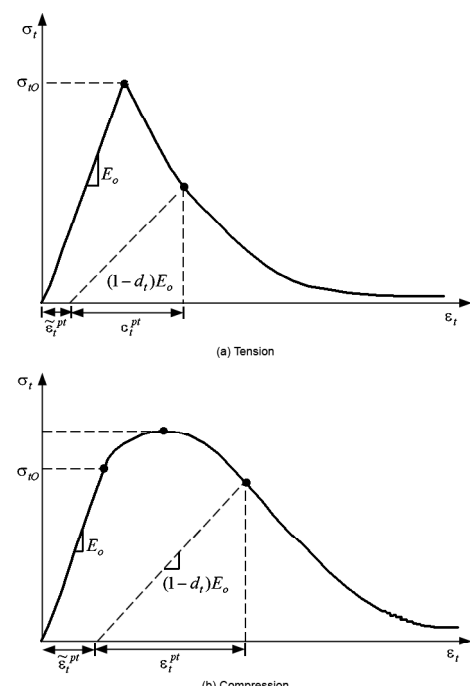
**Figure 9.** The shear capacity curves of the experimental walls.



Figure 10. The crack patterns of the analytical and the experimental models.

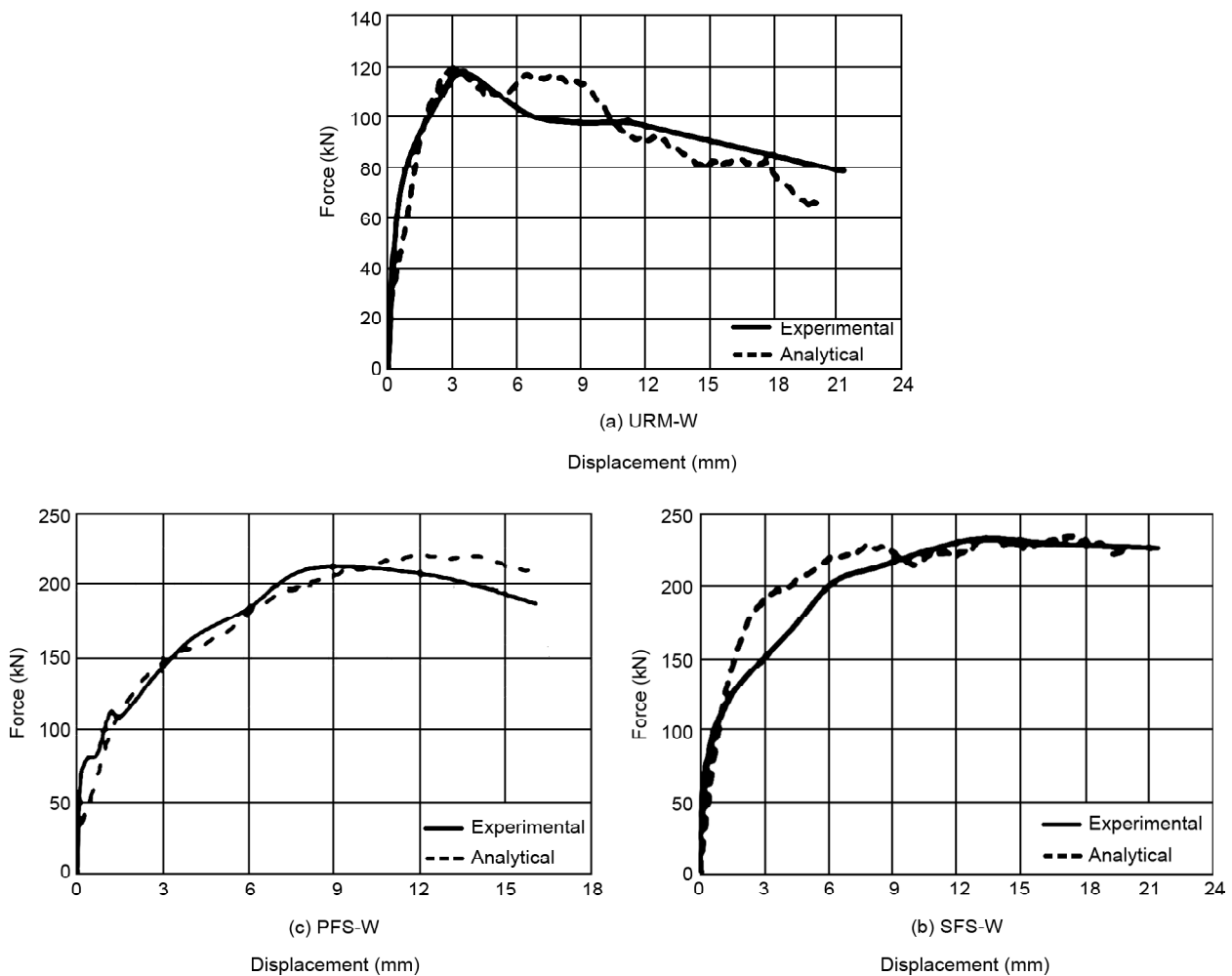


Figure 11. The shear capacity curves of analytical and the experimental models.

7. Conclusions

This paper presents the experimental and analytical results of the in-plane behavior of confined URM walls before and after retrofit using steel-fiber and polypropylene-fiber shotcrete layer in full scale. A prototype wall was tested as a reference wall. The other two walls were retrofitted on one side as described above. Besides, in order to evaluate the crack pattern, the maximum and minimum principal stress contours and shear capacity curves for the specimens, a micro finite element analyses were carried out. The following conclusions can be drawn from the present study:

1. The elastic stiffness of the retrofitted wall with steel-fiber shotcrete is more than the polypropylene-fiber shotcrete. The shear strength of the retrofitted wall with steel-fiber and polypropylene-fiber increase about 98% and 87% respectively, in comparison to URM wall. Moreover, the ductility and the energy dissipation of the SFS-W are more than the PFS-W. Therefore, the steel-fiber shotcrete had a greater influence on the response of the confined URM walls than on the polypropylene-fiber shotcrete.
2. Using mesh-reinforced shotcrete on one side of the wall is effective, but trivial out-of-plane displacements are observed.
3. The pushover analyses on the macro models of the walls are well estimated on the maximum and minimum principal stress contours as well as the first cycle of the capacity curves. The modes of failure are well matched with the mode of failure obtained from the experimental results.

Acknowledgments

The authors would like to acknowledge the financial support of Tehran Province Gas Company.

References

1. Karantoni, F. and Fardis, M. (1992) Effectiveness of seismic strengthening techniques for masonry buildings. *J. Struc. Eng., ASCE*, **118**(7), 1884-1902.
2. Abrams, D.P. and Lynch, J.M. (2001) *Flexural Behavior of Retrofitted Masonry Piers*. KEERC-MAE Joint Seminar on Risk Mitigation for Regions of Moderate Seismicity, Illinois, USA.
3. Abrams, D., Smith, T., Lynch, J., and Franklin, S. (2007) Effectiveness of rehabilitation on seismic behaviour of masonry piers. *Journal of Structural Engineering (ASCE)*, **133**(1), 32-43.
4. Tomazevic, M. (1999) *Earthquake Resistant Design of Masonry Buildings*. Imperial College Press, London, England.
5. Kahn, L. (1984) Shotcrete retrofit for unreinforced brick masonry. *Proceedings of the 8th WCEE*, USA.
6. Ghiassi, B., Soltani, M., and Tasnimi, A.A. (2012) Seismic evaluation of masonry structures strengthened with reinforced concrete layers. *Journal of Structural Engineering (ASCE)*, **138**(6), 729-743.
7. Ezeldin, A.S. and Balaguru, P.N. (1992) Normal and high-strength fiber reinforced concrete under compression. *Journal of Materials in Civil Engineering*, **4**(4), 415-429.
8. Bencardino, F., Rizzuti, L., and Swamy, N. (2008) Stress-strain behaviour of steel fibre-reinforced concrete in compression. *Journal of Materials in Civil Engineering (ASCE)*, **20**(3), 255-263.
9. Beddar, M. (2008) Development of steel fibre reinforced concrete from antiquity until the present day. *Proceedings of the International Conference Concrete: Constructions Sustainable Option*, Dundee, UK, 35-44.
10. Tomazevic, M. (2000) Some aspect of experimental testing of seismic behaviour of masonry walls. *ISET Journal of Earthquake Technology* **40**, *4*, 101-117.
11. Milani, G. (2007) A simple equilibrated homogenization model for the limit analysis of masonry structures. *WSEAS Transactions on Applied and Theoretical Mechanics*, **2**(5), 119-125.
12. Lourenco, P.B. (1996) *Computational Strategies for Masonry Structures*. Ph.D. Thesis, Delft University of Technology, Delft, The Netherlands.
13. Dhanasekar, M. (1985) *The Performance of Brick Masonry Subjected to in Plane Loading*. Ph.D. Thesis, University of Newcastle,

Australia.

14. Zhuge, Y. (1995) *Nonlinear Dynamic Response of Unreinforced Masonry under In Plane Lateral Loads*. Ph.D. Thesis, Queensland University of Technology, Australia.
15. INBC-Part 8, (2005) *Design and Construction of Masonry Buildings*. Iranian National Building Code, Part 8, Ministry of Housing and Urban Development, I.R. Iran.
16. ASTM (2013) *Standard Test Method for Compressive Strength of Hydraulic Cement Mortars*. ASTM C109/C109M-13, West Conshohocken, PA.
17. ASTM. (2009) *Standard Test Methods for in Situ Measurement of Masonry Mortar Joint Shear Strength Index*. ASTM C1531-09, West Conshohocken, PA.
18. ASTM. (2012) *Standard Test Method for Compressive Strength of Cylindrical*. ASTM C39/C39M-12a, West Conshohocken, PA.
19. ASTM. (2012) *Standard Test Method for Sampling and Testing Brick and Structural Clay Tile*. ASTM C67-12, West Conshohocken, PA.
20. *ABAQUS Theory Manual*, version 6.3, Hibbitt Karlson & Sorensen, Inc 2002.
21. Kachanov, L.M. "Ovremenij Razruzenijav Usloviach Polzuesti", Izv. Ak. Nauk CCCP, Otd. Techn. Nauk, nr 8, 1958; 26-31
22. CSI (2006) *Technical Note Material Stress-Strain Curves*. Computers and Structures, INC., Berkeley, California.
23. Maekawa, K., Okamura, H., and Pimanmas, A. (2003) *Non-linear Mechanics of Reinforced Concrete*. Spon Press, New York, USA.